

## Supporting Information

# Tri-cationic copolymer hydrogels with adjustable adhesion and antibacterial properties for flexible wearable sensors

Xiangbin Sun<sup>1a</sup>, Xiaoqing Liu<sup>1a</sup>, Peng Huang<sup>a</sup>, Zeyuan Wang<sup>b</sup>, Yufeng He<sup>a</sup>, Pengfei Song<sup>a</sup>,  
Rongmin Wang<sup>a\*</sup>

<sup>a</sup> Key Lab Eco-functional Polymer Materials of MOE, Institute of Polymer, College of Chemistry & Chemical Engineering, Northwest Normal University, Lanzhou 730070, China. <sup>b</sup> School of Pharmacy, Temple University, Philadelphia, Pennsylvania, 19140, USA. <sup>1</sup>Xiangbin Sun & Xiaoqing Liu are the co-first authors. \*Corresponding authors.

Email: wangrm@nwnu.edu.cn

### The characterization of monomers and intermediates

The <sup>1</sup>H-NMR (400 MHz, DMSO-d<sub>6</sub>) (δ/ppm) results of VPImS were as following: 9.48 (1H, imidazole), 8.18 (1H, imidazole), 7.93 (1H, imidazole), 7.31~7.26 (1H, -CH=CH<sub>2</sub>), 6.96~6.92 (1H, -CH=CHH), 6.40~6.37 (1H, -CH=CHH), 4.34~4.31 (2H, -CH<sub>2</sub>-CH<sub>2</sub>-CH<sub>2</sub>-SO<sub>3</sub><sup>-</sup>), 2.45~2.42 (2H, -CH<sub>2</sub>-CH<sub>2</sub>-CH<sub>2</sub>-SO<sub>3</sub><sup>-</sup>), 2.13~2.10 (2H, -CH<sub>2</sub>-CH<sub>2</sub>-CH<sub>2</sub>-SO<sub>3</sub><sup>-</sup>). <sup>1</sup>H-NMR spectrum was showed in Fig. S1.

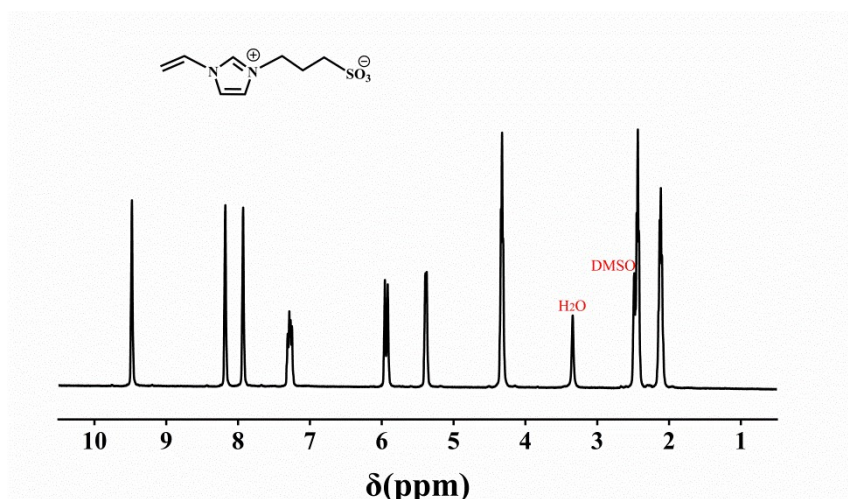
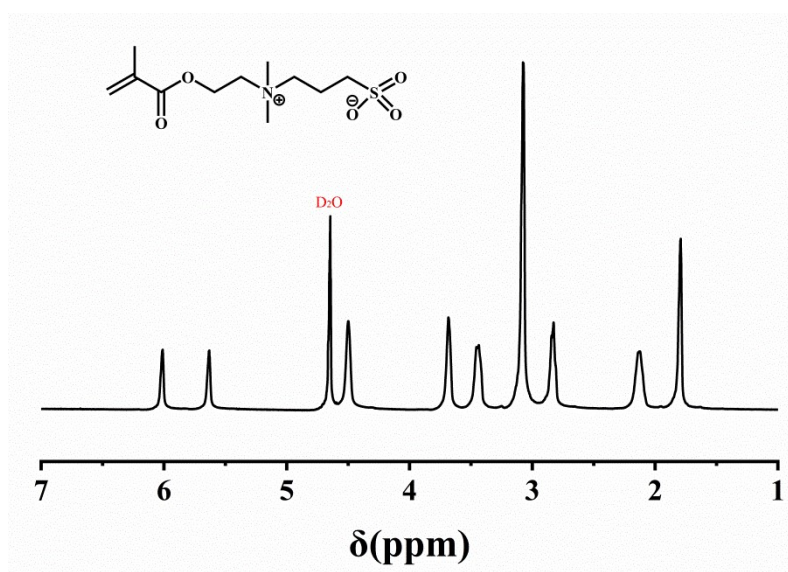


Fig. S1. <sup>1</sup>H-NMR spectrum of VPImS.

The <sup>1</sup>H-NMR (400 MHz, D<sub>2</sub>O) (δ/ppm) results of MASB were as following: 6.11 (1H, CHH=C(CH<sub>3</sub>)-), 5.72 (1H, CHH=C(CH<sub>3</sub>)-), 4.59 (2H, -OCO-CH<sub>2</sub>-), 3.77 (2H, -OCOCH<sub>2</sub>CH<sub>2</sub>N(CH<sub>3</sub>)-), 3.53 (2H, -N(CH<sub>3</sub>)<sub>2</sub>CH<sub>2</sub>-), 3.17 (6H, -N(CH<sub>3</sub>)<sub>2</sub>-), 2.92 (2H, -CH<sub>2</sub>-SO<sub>3</sub><sup>-</sup>),

2.22 (2H,  $-\text{CH}_2\text{CH}_2\text{CH}_2\text{SO}_3^-$ ), 1.88 (3H,  $\text{CH}_2=\text{C}(\text{CH}_3)-$ ). And  $^1\text{H-NMR}$  spectrum was showed in Fig. S2.



**Fig. S2.**  $^1\text{H-NMR}$  spectrum of MASB.

**Table S1.** The recipe for synthesis of TCPHS with different ratio of VPIImS/MASB.

Entry	VPIImS (mmol)	MASB (mmol)	VPIImS/MASB	APMaC (mmol)	MBAA (mmol)	Product
1	0	7.5	-	10.0	0.1	P(MAM)
2	12.5	2.5	5:1	5.0	0.1	TCPHS <sub>1</sub>
3	10.0	5.0	2:1	5.0	0.1	TCPHS <sub>2</sub>
4	7.5	7.5	1:1	5.0	0.1	TCPHS <sub>3</sub>
5	5.0	10.0	0.5:1	5.0	0.1	TCPHS <sub>4</sub>
6	2.5	12.5	0.2:1	5.0	0.1	TCPHS <sub>5</sub>

**Table S2.** The recipe for synthesis of TCPHs with different amount of APMaC.

Entry	VPImS (mmol)	MASB (mmol)	APMaC (mmol)	MBAA (mmol)	Product
7	7.5	7.5	5.0	0.1	TCPH <sub>S3</sub>
8	7.5	7.5	7.5	0.1	TCPH <sub>S6</sub>
9	7.5	7.5	10.0	0.1	TCPH <sub>S</sub>
10	7.5	7.5	12.5	0.1	TCPH <sub>S8</sub>
11	7.5	7.5	15.0	0.1	TCPH <sub>S9</sub>

**Table S3.** The recipe for synthesis of TCPHs with different amount of MBAA

Entry	VPImS (mmol)	MASB (mmol)	APMaC (mmol)	MBAA (mmol)	Product
12	7.5	7.5	10.0	0.20	TCPH <sub>S10</sub>
13	7.5	7.5	10.0	0.15	TCPH <sub>S11</sub>
14	7.5	7.5	10.0	0.10	TCPH <sub>S</sub>
15	7.5	7.5	10.0	0.05	TCPH <sub>S12</sub>

### Measurement of antibacterial property and biocompatibility

The antibacterial properties of hydrogels were studied from two aspects of bactericidal property<sup>[1]</sup> and anti-bacterial adhesion<sup>[2]</sup>. Normal mouse fibroblast L9292 was used to evaluate biocompatibility of hydrogels in vitro by standard MTT method<sup>[3]</sup>.

#### Bactericidal property

*E. coli* and *S. aureus* were selected as representatives to test the bactericidal activity of TCPoGs. The hydrogel preform solution was poured into circular die to make a wafer (height: 1 mm; diameter: 10 mm). The sterilized hydrogels and activated bacterial suspension were added into phosphate buffer solution (PBS). The bacterial suspension was spread on the nutrient agar plate and incubated in biochemical incubator at 37 °C for 48 hrs to observe the growth of colonies.

## Anti-bacterial adhesion

Firstly, the sterilized TCPHs hydrogel and polyacrylamide (PAM) hydrogel were immersed in bacterial suspension and cultivated at 37 °C. Secondly, the hydrogels surface was washed with PBS to remove bacteria that did not adhere to the sample surface. Then, the bacterial adhesion on the hydrogel surface was observed by fluorescence microscope (DM5000B, Leica).

## Biocompatibility

The TCPHs extract was obtained by soaking the sterilized hydrogels in the culture medium overnight. The cells and culture medium were seeded in 96-well plates and incubated in a thermostat (5% CO<sub>2</sub>, 37°C and saturated humidity). The TCPHs extract was used to replace the culture medium, and MTT was added into each well to detect the optical density at 600 nm. The cells without being treated was recorded as the control group.

## Measurement of electrical property and sensing behavior

### Electrical test

Using TCPHs as conductor, a LED and an external power supply was used to form a complete circuit. By observing the brightness of LED in different states (original, stretch and cut), the conductivity of the hydrogels was judged. The resistance of TCPHs was obtained by digital source table (Keithley 2450). The conductivity ( $\sigma$ ), relative resistance ( $\Delta R/R_1\%$ ) and the gauge factor (GF) of TCPHs could be calculated by formula (1) ~ formula (3)

$$\sigma = \frac{L}{W \times T} \times \frac{1}{R} \quad (1)$$

where L, W and T were the length, width and thickness of the hydrogels, and R represented resistance of the hydrogels.

$$\frac{\Delta R}{R_1}\% = \frac{R_2 - R_1}{R_1} \times 100\% \quad (2)$$

$$GF = \left[ \frac{R_2 - R_1}{R_1} \right] / \varepsilon \quad (3)$$

where  $R_1$  was the resistances of the original hydrogels,  $R_2$  was the resistance of the hydrogels when it was stretched or compressed, and  $\epsilon$  was the strain of the hydrogels.

### Sensing behavior test

The hydrogels was adhere to different parts of the human body, and the real-time resistance of TCPHs during human movement was recorded using digital source table. Different body movements could be monitored by identifying the waveform and intensity of the output signal of the relative resistance-time curve.

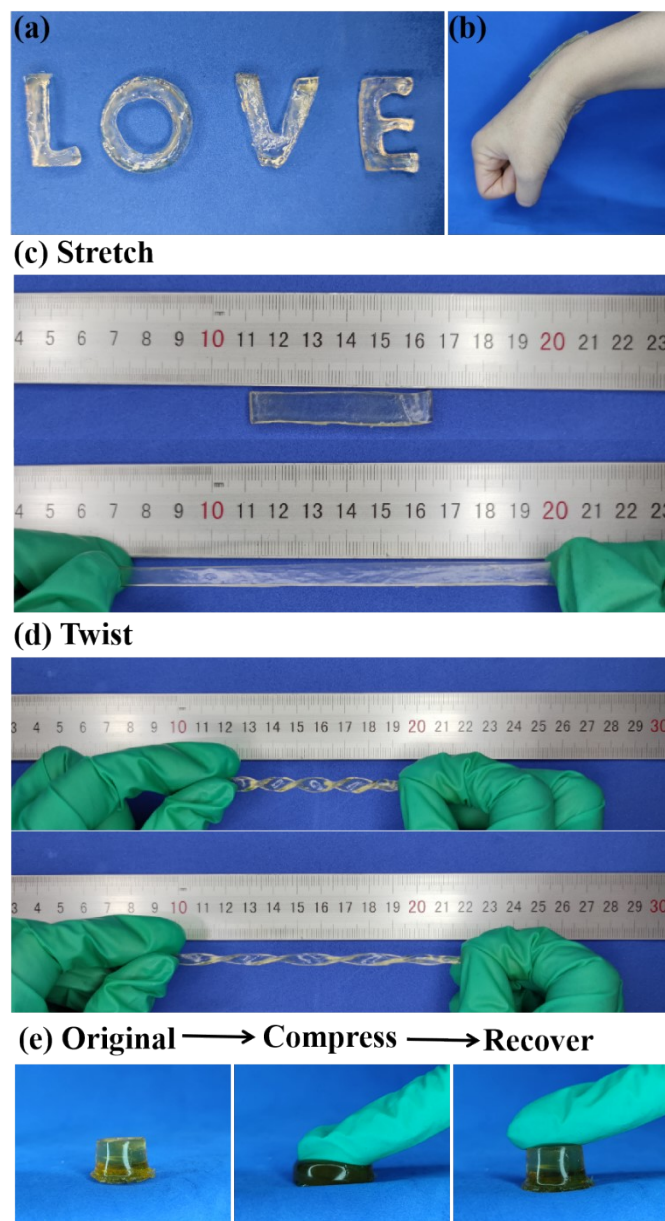


Fig. S3. Digital images of the TCPHs with different morphology.

## NMR spectra

The  $^{13}\text{C}$ -SSNMR spectrum of TCPHs was shown in Fig. S4. The proton chemical shift of carbonyl appeared at 178.37 ppm. The peaks at 137.70 ppm and 124.38 ppm were attributed to the characteristic peaks of imidazole ring. The proton chemical shift of methyl group at the end of quaternary ammonium salt appeared at 53.97 ppm. The other peaks have compared with the reported polycationic hydrogel,<sup>[4]</sup> which proved that TCPHs had been successfully synthesized.

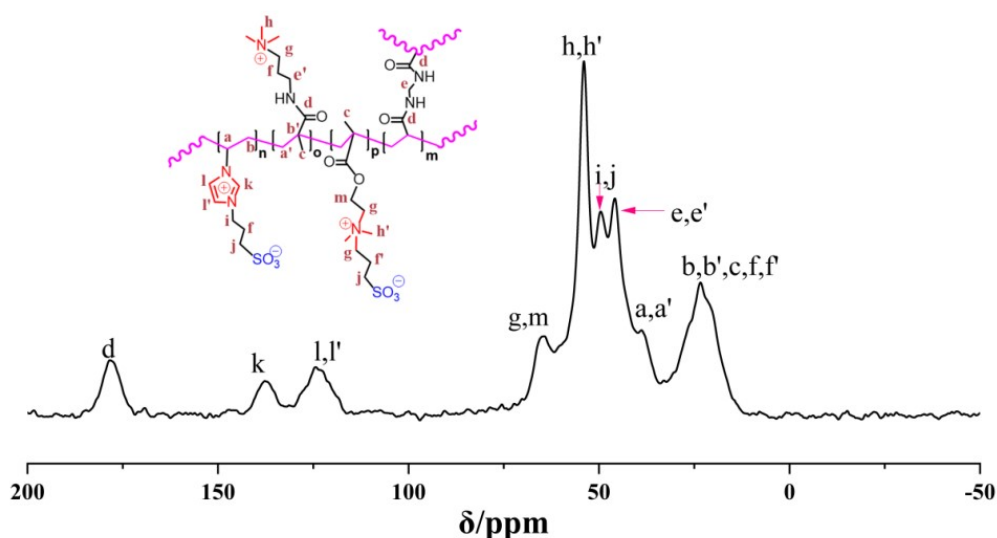


Fig. S4.  $^{13}\text{C}$ -SSNMR of TCPHs.

## IR spectra

TCPHs was further confirmed by FT-IR spectroscopy, and compared with P(VAM) and zwitterionic MASB. In P(VAM), the stretching vibration of -NH appeared at  $3438\text{ cm}^{-1}$ , and the peaks at  $3032\text{ cm}^{-1}$  and  $2956\text{ cm}^{-1}$  were related to the unsaturated and saturated stretching vibration absorption peaks of C-H, respectively. The stretching vibration absorption peak of carbonyl (C=O) in amide was located at  $1645\text{ cm}^{-1}$ . The absorption peaks at  $1533\text{ cm}^{-1}$ ,  $1484\text{ cm}^{-1}$  and  $1204\text{ cm}^{-1}$  were attributed to the characteristic absorption peaks of amide. In addition, the stretching vibration of C-H in imidazole was occurred to  $3138\text{ cm}^{-1}$ . The absorption peaks at  $1568\text{ cm}^{-1}$  and  $1456\text{ cm}^{-1}$  were arranged to the skeletal vibration of imidazole. The strong infrared absorption peaks at  $1178\text{ cm}^{-1}$  and  $1035\text{ cm}^{-1}$  were attributed to the sulfonate

(-SO<sub>3</sub><sup>-</sup>). In addition to the above characteristic absorption peaks in TCPHs, there was a peak at 1731 cm<sup>-1</sup>, which belonged to the ester carbonyl (O-C=O) in MASB structural unit. It was confirmed that TCPHs was successfully prepared.

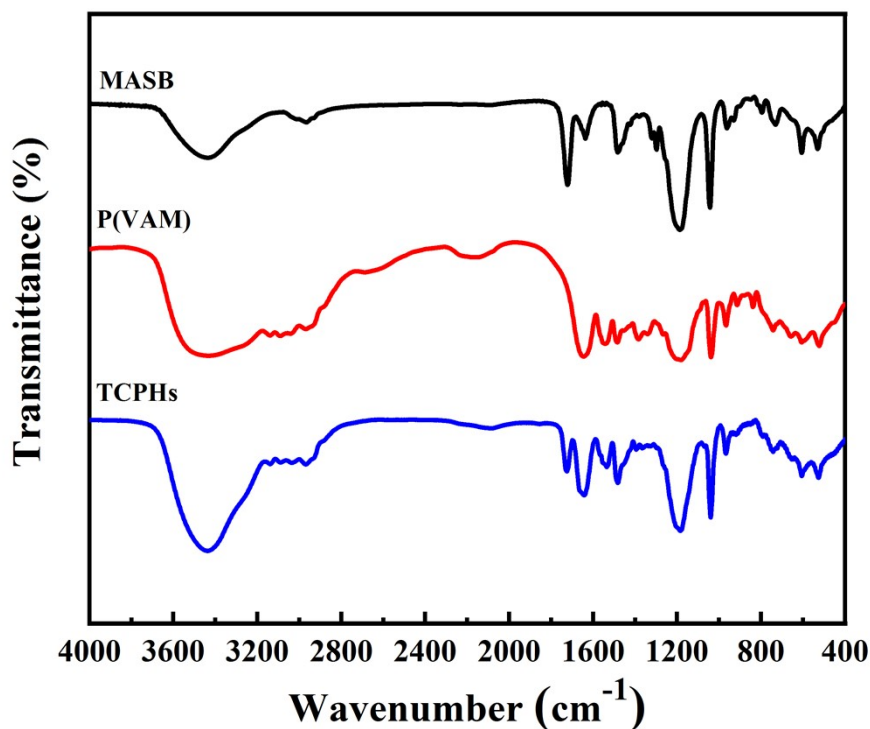


Fig. S5. FT-IR spectra of TCPHs, P(VAM) and zwitterionic MASB.

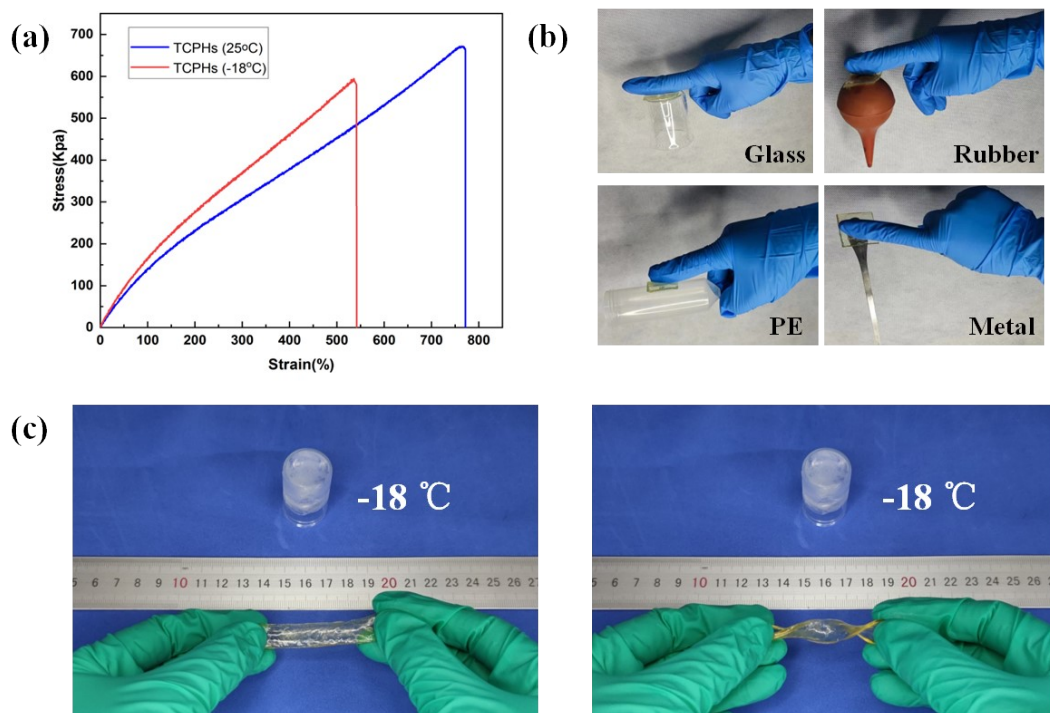


Fig. S6. TCPHs stored at -18 °C for 24 h: (a) tensile property, (b) adhesion property,

(c) resistance to twisted

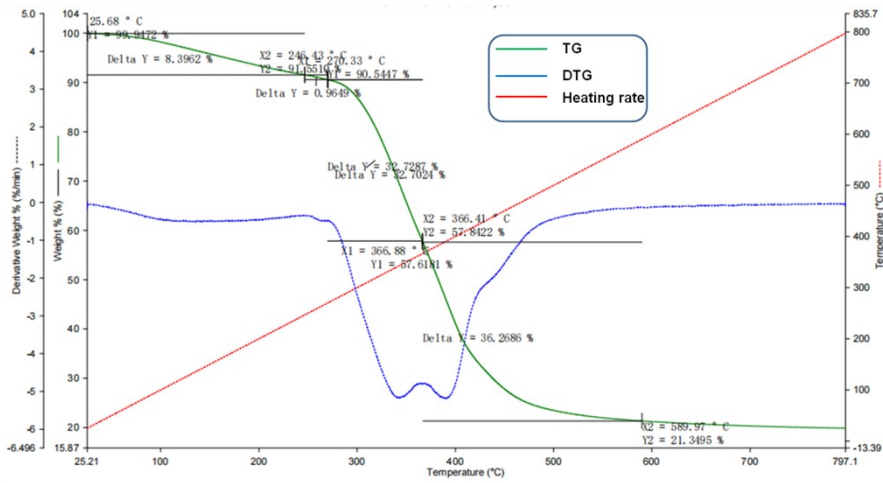


Fig. S7a. The TG curve of TCPHs

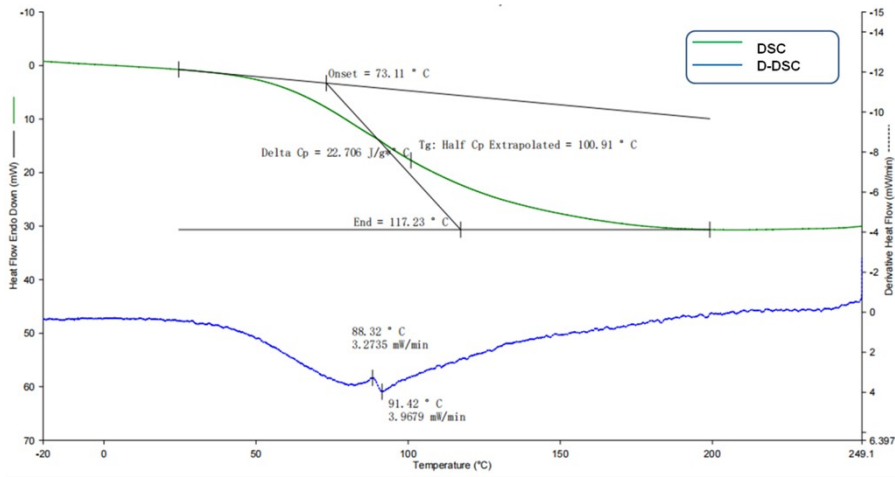


Fig. S7b. The DSC curve of TCPHs

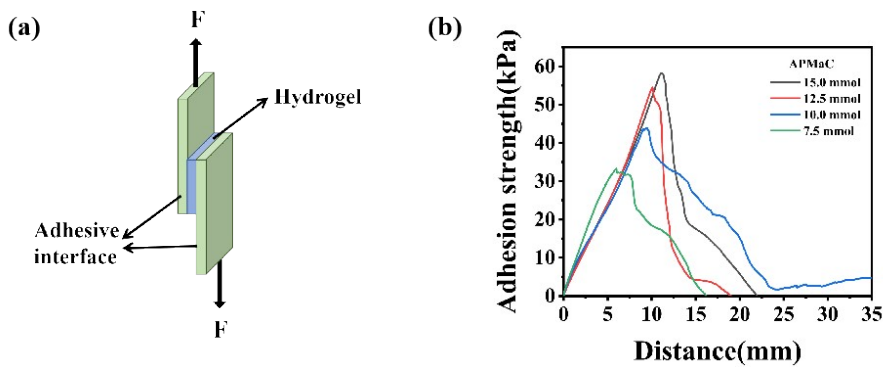


Fig. S8. (a) Schematic illustration of lap shear test, (b) relationship between the adhesion strength and distance with different amount of APMaC in TCPHs.

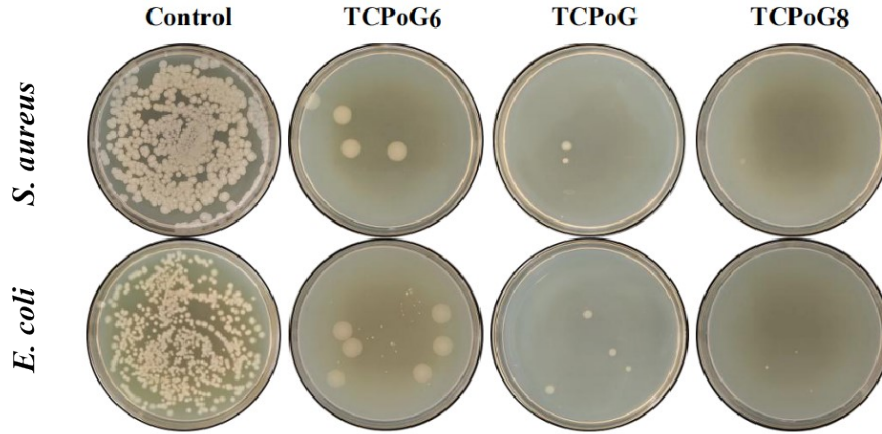


Fig. S9. Bactericidal performance of TCPHs

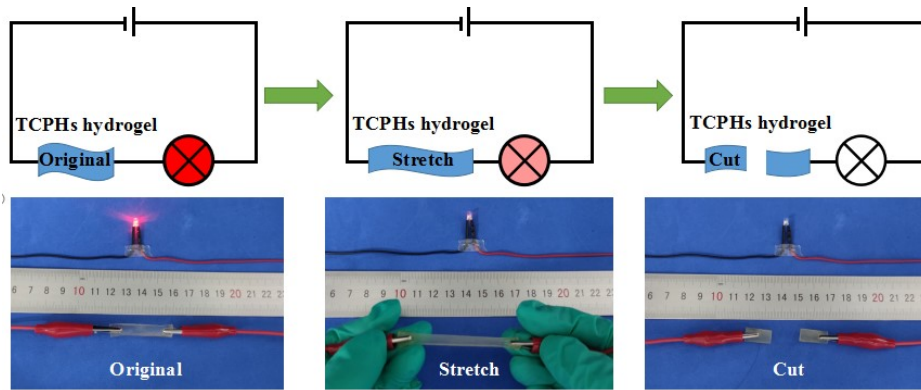


Fig. S10. Conductivity of TCPHs in different states: (a) original, (b) stretch, (c) cut.

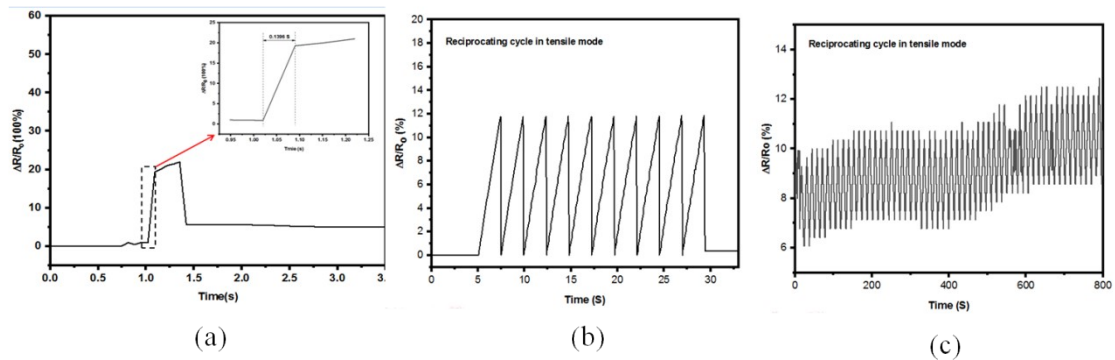
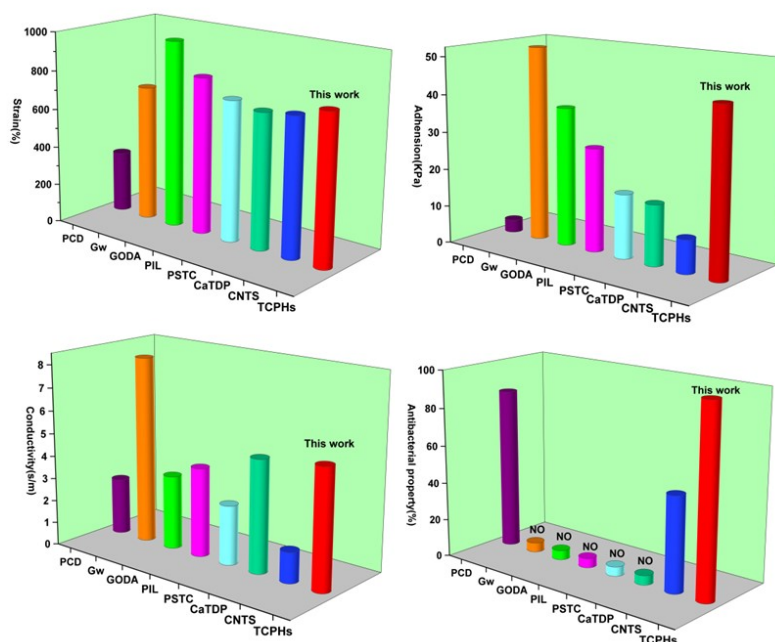


Fig. S11. (a) Response time, (b) low detection line, and (c) impedance stability after 100 cycles



**Fig. S12. Quantitative comparison of various hydrogels**

## Caption of videos

**Video S1:** The flexibility of TCPHs after being frozen at -18 °C for 24 hrs.

**Video S2:** Adhesive property of TCPHs.

**Video S3:** Conductivity sensitivity of TCPHs.

## References

- [1] T. Dai, C. Wang, Y. Wang, W. Xu, J. Hu, Y. Cheng. A nanocomposite hydrogel with potent and broad-spectrum antibacterial activity. *ACS Appl. Mater. Interfaces.*, 10(2018): 15163-15173.
- [2] J. Yan, Y. Ji, M. Huang, T. Li, Y. Liu, S. Lü, M. Liu. Nucleobase-inspired self-adhesive and inherently antibacterial hydrogel for wound dressing. *ACS Materials Lett.*, 2(2020), 1375-1380.
- [3] Fang, Y., Xing, C., Liu, J., Zhang, Y., Li, M., Han, Q. Supermolecular film crosslinked by polyoxometalate and chitosan with superior antimicrobial effect. *Int. J. Biol. Macromol.*, 154(2020), 732-738.
- [4] X. Liu, P. Huang, J. Wang, X. Wang, Y. He, P. Song, R. Wang. Rational design of

polycationic hydrogel with excellent combination functions for flexible wearable electronic devices. *Macromol. Mater. Eng.*, 307(2021), 2100593.